

## Hydrothermal Preparation of Biomineral Botallackite $\text{Cu}_2(\text{OH})_3\text{Cl}$ Hollow Nanoarchitectures

Zhitao Chen and Lian Gao\*

State Key Laboratory of High Performance Ceramics and Superfine Microstructure, Shanghai Institute of Ceramics, Chinese Academy of Sciences, Shanghai 200050, P. R. China

(Received March 3, 2008; CL-080235; E-mail: liangaoc@online.sh.cn)

A novel and facile way to produce botallackite ( $\text{Cu}_2(\text{OH})_3\text{Cl}$ ) flower-like solid and hollow architectures with an average diameter of 400 nm is put forward, meanwhile, its probable reaction mechanism is also discussed.

Hierarchical nanostructures with well-defined outer and inner structure using nanoparticles, nanoplates, nanorods, and nanochains as building blocks have attracted great interest owing to their many novel properties and potential applications.<sup>1</sup> In addition to common three-dimensional architectures, controlled structures of building units in curved organizations remain an important challenge for material self-assembly, as hollow structures are highly promising in new technological applications, including the delivery of drugs, catalysis, chemical storage, and microcapsule reactors as building blocks in the fabrication of photonic band gap crystals.<sup>2</sup>

Basic copper(II) chloride of stoichiometry  $\text{Cu}_2(\text{OH})_3\text{Cl}$  is found in four naturally occurring phases, atacamite (orthorhombic), botallackite (monoclinic), clinoatacamite, and paratacamite (rhombohedral).<sup>3</sup> The synthesis of atacamite  $\text{Cu}_2(\text{OH})_3\text{Cl}$  relies mainly two methods: chemical reaction of an alkaline solution with an aqueous solution and direct precipitation by using copper chloride as reagent.<sup>4</sup> Until now, much research has been undertaken on the mineral properties of atacamite  $\text{Cu}_2(\text{OH})_3\text{Cl}$ .<sup>5</sup> Concerning the morphology control of  $\text{Cu}_2(\text{OH})_3\text{Cl}$ , Zhu et al. have prepared  $\text{Cu}_2(\text{OH})_3\text{Cl}$  nanoribbons and Kratochvil and Matijevic have made bipyramidal  $\text{Cu}_2(\text{OH})_3\text{Cl}$  microparticles.<sup>6</sup> To our best knowledge, there is no report of the control of the hollow flower-like architectures of  $\text{Cu}_2(\text{OH})_3\text{Cl}$ .

In this work, we report a novel and simple method of conversion of  $\text{Cu}(\text{NH}_3)_4^{2+}$  to atacamite  $\text{Cu}_2(\text{OH})_3\text{Cl}$  hollow flower-like structures under cetyltrimethylammonium bromide (CTAB)-assisted hydrothermal conditions. By adjusting the reaction conditions, we obtained well-defined hollow spheres in high yield, even up to 100%. Moreover, we investigated the growth process of hollow spheres.

All of the reagents (analytical reagent) were purchased from SCRC Chemical Co., Ltd. (China) and used without further purification. Two starting aqueous solutions,  $\text{CuCl}_2$  (0.2 M) and  $\text{NH}_3 \cdot \text{H}_2\text{O}$  (4 M) were prepared. Aqueous ammonia was added dropwise to a copper(II) chloride solution to adjust the pH value to 12 under vigorous stirring. In a typical experimental procedure, 7 mL of this mixture was mixed with 70 mL of anhydrous ethanol, meanwhile 0.2 g of CTAB was added to this ethanol-water solution under vigorous stirring. The latter mixture was transferred into a 80-mL Teflon-lined autoclave, then, the autoclave was maintained at 180 °C for 3–12 h and cooled down to room temperature on standing. Blue precipitate was collected and rinsed several times. Finally, the products were obtained by centrifugation and drying in vacuum at 60 °C.

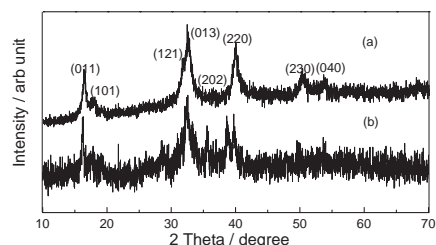


**Figure 1.** The XRD pattern of  $\text{Cu}_2(\text{OH})_3\text{Cl}$  samples (a) 180 °C for 12 h (b) 180 °C for 6 h.

The as-prepared  $\text{Cu}_2(\text{OH})_3\text{Cl}$  hollow flower-like structures were structurally characterized by X-ray diffraction, indicating an orthorhombic structure with low crystallinity. The typical XRD patterns of  $\text{Cu}_2(\text{OH})_3\text{Cl}$  hollow flower-like structures is illustrated in Figure 1 with all diffraction peaks well indexed to orthorhombic phase  $\text{Cu}_2(\text{OH})_3\text{Cl}$  with JCPDS card No. 78-0372. It is found that with prolonging reaction time, the crystallization of  $\text{Cu}_2(\text{OH})_3\text{Cl}$  with hollow flower-like structures is improved obviously.

The morphologies of the  $\text{Cu}_2(\text{OH})_3\text{Cl}$  hollow structures obtained under typical conditions were examined using TEM analysis. As shown in Figure 2a, the morphology of the  $\text{Cu}_2(\text{OH})_3\text{Cl}$  architectures at the first stage (3 h reaction time) is flower-like nanostructure. And the diameters of  $\text{Cu}_2(\text{OH})_3\text{Cl}$  architectures ranged from 0.2 to 0.3  $\mu\text{m}$  which are composed of nanometer plates. Typical TEM image of products at the sec-

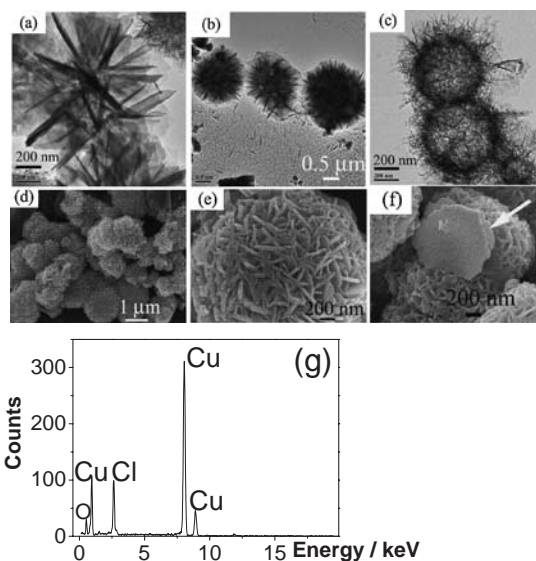


**Figure 2.** Morphology of the product. (a) TEM image of the samples. (b), (c) Typical magnified TEM image of flower-like architecture and hollow spheres. (d)–(f) SEM images of the samples. (g) The EDS spectrum of hollow spheres.

ond stage (6 h reaction time) is shown in Figure 2b, which discloses the hedgehog-like structure of  $\text{Cu}_2(\text{OH})_3\text{Cl}$  with a diameter of  $0.5\ \mu\text{m}$ . In Figure 2c, hollow spheres of  $\text{Cu}_2(\text{OH})_3\text{Cl}$  is the dominant morphology, which is the third stage product at 12 h reaction time. The diameter of the hollow spheres is about  $400\ \text{nm}$ , which is consistent with the size of the hedgehog-like product in the second stage. The hollow spheres may have promising applications in drug delivery and microchemical reactors owing to their hollow space with an inner diameter of  $0.4\ \mu\text{m}$ . As shown in the FE-SEM image in Figure 2d, the panoramic morphology of the  $\text{Cu}_2(\text{OH})_3\text{Cl}$  is spherical with diameters ranging from  $0.3$  to  $0.5\ \mu\text{m}$ , which corresponds to the TEM results in Figure 2b. From the magnified SEM images, we can see that the surfaces of spheres are constructed by nanosheets as shown in Figure 2e, which is also confirmed by TEM observation. Interestingly, these nanoplates assemble into a hedgehog-like structure. Moreover, the hedgehog-like structure consisting of plates is confirmed by another typical SEM image (Figure 2f), which provided an illumination to see the plates. These observations indicate that a high yield of hedgehog-like  $\text{Cu}_2(\text{OH})_3\text{Cl}$  can be achieved under the present experimental conditions. The composition of product was confirmed by using EDS analysis. In the EDS spectrum of typical product, the peaks of Cu, O, and Cl are clearly observed without any other peaks (the Cu peaks in the spectrum also contained the background from the copper TEM grid), which confirm the formation of pure  $\text{Cu}_2(\text{OH})_3\text{Cl}$  (Figure 2g).

Based on these observations, a base-erosion mechanism to form hollow  $\text{Cu}_2(\text{OH})_3\text{Cl}$  structure was proposed, with reference to the preparation of multiped-like CuO and tubular CuO. The schematic representation of the formation mechanism of hollow  $\text{Cu}_2(\text{OH})_3\text{Cl}$  structure is shown in Figure 3. After formation of  $\text{Cu}_2(\text{OH})_3\text{Cl}$  nanoplate with large diameter in step A,  $\text{Cu}_2(\text{OH})_3\text{Cl}$  nanosheet with small size adhered to the nanoplate. At step B, the center of the  $\text{Cu}_2(\text{OH})_3\text{Cl}$  nanoarchitecture became thicker and thicker, and the outer layer became ordered gradually. A similar phenomenon has been observed in our previous research.<sup>7</sup> Along with the increase of reaction time, the core of the nanoarchitecture was consumed gradually. At the most important step (step C) to hollow  $\text{Cu}_2(\text{OH})_3\text{Cl}$  structure, the existence of large amounts of  $\text{NH}_3$  and a gas-liquid equilibrium in the autoclave is the key factor, which makes the nanoplates erode from the center point to outside gradually.<sup>7</sup> When the reaction time was prolonged to 12 h, the core of the nanoarchitecture became thinner.

We did further control experiments which were carried out to investigate the effect of the amount of ammonia and the exist-

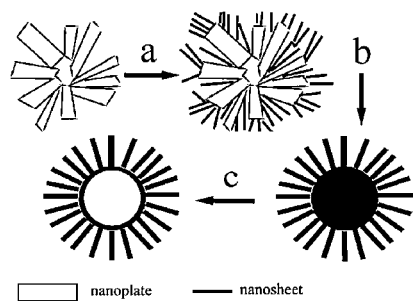


**Figure 3.** Schematic representation of the formation of  $\text{Cu}_2(\text{OH})_3\text{Cl}$  hollow structure.

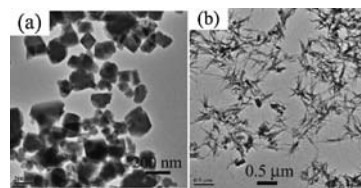


**Figure 4.** (a) TEM image of sample when the pH value of initial mixture is 11. (b) TEM image of sample prepared with a CTAB-absent reaction system.

tence of CTAB. The amount of ammonia corresponded to the pH value of the  $\text{Cu}(\text{NH}_3)_4^{2+}$  precursor. Under conditions of less ammonia, we obtained a morphology of short rods and blocks, which is shown in Figure 4a. So an appropriate amount of ammonia is the key factor to form  $\text{Cu}_2(\text{OH})_3\text{Cl}$  hollow architectures. Moreover, we attempted the reaction without CTAB. As shown in Figure 4b, the main morphology of  $\text{Cu}_2(\text{OH})_3\text{Cl}$  was thread-like. CTAB is a cationic surfactant, then CTAB can be combined with the  $\text{OH}^-$  and  $\text{Cl}^-$  easier than  $\text{Cu}(\text{NH}_3)_4^{2+}$ , affecting the kinetics process. The effect of CTAB depends on the formation of a complex between the CTAB and the negative ion in the reaction system.<sup>8</sup>

In summary, a novel and simple approach was successfully developed to make  $\text{Cu}_2(\text{OH})_3\text{Cl}$  hollow flower-like structures with diameter of  $500\ \text{nm}$ . Control experiments demonstrated that the pH value of mixture and the addition of CTAB played important functions in the formation of hollow structures. Based on the results of control experiments, we put forward a mechanism for the formation of hollow structures. Because of the simple reaction process, this method can also be expected to gain success in preparation of other oxide hollow spheres.

## References

- 1 T. D. Ewers, A. K. Sra, B. C. Norris, R. E. Cable, C.-H. Cheng, D. F. Shantz, R. E. Schaak, *Chem. Mater.* **2005**, *17*, 514; X. Yang, Y. Makita, Z.-H. Liu, K. Sakane, K. Ooi, *Chem. Mater.* **2004**, *16*, 5581; H. G. Yang, H. C. Zeng, *Angew. Chem., Int. Ed.* **2004**, *43*, 5930; B. Liu, H. C. Zeng, *J. Am. Chem. Soc.* **2004**, *126*, 8124; S. Chen, Z. Fan, D. L. Carroll, *J. Phys. Chem. B* **2002**, *106*, 10777.
- 2 F. Caruso, R. A. Caruso, H. Mohwald, *Science* **1998**, *282*, 1111; F. Caruso, *Adv. Mater.* **2001**, *13*, 11; J. Goldberger, R. He, Y. Zhang, S. Lee, H. Yan, H.-J. Choi, P. Yang, *Nature* **2003**, *422*, 599; Y. Sun, Y. Xia, *Science* **2002**, *298*, 2176; B. T. Holland, C. F. Blanford, A. Stein, *Science* **1998**, *281*, 538.
- 3 A. M. Pollard, R. G. Thomas, P. A. Williams, *Mineral. Mag.* **1989**, *53*, 557.
- 4 X. Wen, W. Zhang, S. Yang, *Nano Lett.* **2002**, *2*, 1397.
- 5 R. M. Garrels, R. M. Dreyer, *Geol. Soc. Am. Bull.* **1952**, *63*, 325; H. R. Oswald, W. Feitknecht, *Helv. Chim. Acta* **1964**, *47*, 272; T. L. Woods, R. M. Garrels, *Econ. Geol.* **1986**, *81*, 1989.
- 6 C. L. Zhu, C. N. Chen, L. Y. Hao, Y. Hu, Z. Y. Chen, *J. Cryst. Growth* **2004**, *263*, 473; S. Kratochvil, E. Matijevic, *J. Mater. Res.* **1991**, *6*, 766.
- 7 Z. Chen, L. Gao, *Cryst. Growth Des.* **2008**, *8*, 460; C. Yan, D. Xue, *J. Phys. Chem. B* **2006**, *110*, 11076; S. Konar, Z. R. Tian, *J. Phys. Chem. B* **2006**, *110*, 4054; J. Zhang, L. Sun, C. Liao, C. Yan, *Chem. Commun.* **2002**, 262; Z. Hu, G. Oskam, P. C. Searson, *J. Colloid Interface Sci.* **2003**, *263*, 454.
- 8 E. D. Rosa, S. Sepulveda-Guzman, B. Reesja-Jayan, A. Torres, P. Salas, N. Elizondo, M. J. Yacamán, *J. Phys. Chem. C* **2007**, *111*, 8489.